White Rose Research Online

eprints@whiterose.ac.uk
https://eprints.whiterose.ac.uk
Universities of Leeds, Sheffield and York

Deposited via The University of Leeds.

White Rose Research Online URL for this paper:
https://eprints.whiterose.ac.uk/id/eprint/112201/

Version: Accepted Version

Article:
Low, JE, Loveridge, FA and Powrie, W (2017) Error analysis of the thermal cell for soil thermal conductivity measurement. Proceedings of the Institution of Civil Engineers: Geotechnical Engineering, 170 (GE3). pp. 191-200. ISSN: 1353-2618

https://doi.org/10.1680/jgeen.16.00137

© ICE Publishing. This is an author produced version of a paper published in Proceedings of the Institution of Civil Engineers: Geotechnical Engineering. Uploaded in accordance with the publisher's self-archiving policy.

Reuse
Items deposited in White Rose Research Online are protected by copyright, with all rights reserved unless indicated otherwise. They may be downloaded and/or printed for private study, or other acts as permitted by national copyright laws. The publisher or other rights holders may allow further reproduction and re-use of the full text version. This is indicated by the licence information on the White Rose Research Online record for the item.

Takedown
If you consider content in White Rose Research Online to be in breach of UK law, please notify us by emailing eprints@whiterose.ac.uk including the URL of the record and the reason for the withdrawal request.

UNIVERSITY OF LEEDS
University of Sheffield
UNIVERSITY of York

Error analysis of the thermal cell for soil thermal conductivity measurement

J. E. Low MEng PhD, Max Fordham (formerly University of Southampton)

F. A. Loveridge* BA MSc PhD, CEng, MICE, FGS, CGeol, Royal Academy of Engineering Research Fellow, University of Leeds (formerly University of Southampton)

W. Powrie FREng MA PhD, CEng, FICE, Dean Faculty of Engineering and the Environment & Professor of Geotechnical Engineering, University of Southampton

* corresponding author – F.A.Loveridge@leeds.ac.uk; University of Leeds, Woodhouse Lane, Leeds, UK

Date of revision: 4th July 2016

Number of words in main text: 4628

4 Tables and 14 Figures

Abstract

Soil thermal conductivity is an important factor in the design of energy foundations and other ground heat exchanger systems. Laboratory tests in a thermal cell are often used to determine the thermal conductivity of soil specimens. Two interpretation methods have been suggested. Analysis can be based on the assumption of one-directional heat flow and the thermal conductivity calculated using Fourier's Law. Alternatively the lumped capacitance method can be employed, using results generated as a specimen cools. In this study, six samples of London Clay were tested using a thermal cell. A finite element model of the tests was then used to determine the validity of the assumptions made in analysis. The model showed substantial heat loss through the sides of the specimens, which would impact significantly on the calculated thermal conductivity. The conditions required for the lumped capacitance method to be valid were also found not to be met. Consequently neither analysis method is recommended. A better approach would be to pursue apparatus with fewer heat losses or transient testing techniques.

Notation

A	area (m^2)
Bi	Biot number (dimensionless)
c_p	specific heat capacity (J/kgK)
h	heat transfer coefficient (W/m^2K)
L	length (m)
m	mass (kg)
Q	heat flux (W)
$\dot{Q}$	heat flux per unit volume (W/m^3)
T	temperature (degrees)
t	time (s)
λ	thermal conductivity (W/mK)
ρ	density (kg/m^3)

Keywords

thermal conductivity, soil, thermal cell, ground source heat pumps

Error analysis of the thermal cell for soil thermal conductivity measurement

1 Introduction

Ground source heat pump (GSHP) systems provide a viable alternative to conventional heating and cooling systems in the move towards more sustainable building solutions (Banks, 2008). Heat is transferred between the ground and the building by means of a heat transfer fluid, which is pumped through a series of pipes buried in the ground. To minimise initial construction costs, the pipes may be cast into the foundations, thereby eliminating the need to make further excavations. These systems are known as energy or thermal foundations. To design such a system, it is important to model accurately the heat transfer process between the foundations and the soil. An important input parameter for such analysis is the soil thermal conductivity.

There are several different laboratory methods for measuring soil thermal conductivity e.g. Mitchell & Kao (1978), Farouki (1986). All of them fall into one of two categories, based on analysis of steady-state or transient data. At the laboratory scale, steady-state methods involve applying one-directional heat flow to a specimen and measuring the power input and temperature difference across it when a steady state is reached. The thermal conductivity is then calculated directly using Fourier's Law. Transient methods involve applying heat to the specimen and monitoring temperature changes over time. The transient data are used to determine the thermal conductivity, usually by application of an analytical solution to the heat diffusion equation. Some transient methods can also be used to assess other thermal properties such as thermal diffusivity (Bristow et al, 1994).

A steady-state method that has shown promise is the thermal cell method (Clarke et al, 2008). The main advantage of this method is that it requires minimal preparation for testing U100 (undisturbed, 100 mm diameter) samples of soil taken from routine site investigations. In this paper, the theory and experimental method are described and the limitations discussed. One particular area of concern is heat loss through the apparatus. This is investigated by modelling the thermal cell using finite element analysis, and comparing the results with models of an ideal heat lossless thermal cell.

2 Theory

The thermal cell used in this research (Figure 1a, Table 1) is based on a design and specification by Clarke et al (2008) (Figure 1b). Although other arrangements of thermal cell are used in research, e.g. Alrtimi et al (2013), the Clarke et al (2008) specification is recommended for laboratory soil thermal conductivity testing by the Ground Source Heat Pump Association (GSHPA, 2012) and remains in use in practice. In the Clarke et al (2008) method, the thermal conductivity of a 100 mm diameter 100mm high specimen is measured by generating one-directional heat flow along the axis. In both cases the heat source is a cartridge heater embedded in the lower aluminium platen. Provided that the specimen is well insulated

so that heat losses through the insulation and acrylic base can be neglected, steady heat flow through the specimen is governed by Fourier's Law:

$$\boldsymbol{Q = -\lambda A \frac{\Delta T}{L}} \qquad \textbf{Equation 1}$$

where Q is the power input, A is the cross-sectional area, ΔT is the temperature difference across the length of the specimen, and L is the length of the specimen. In applying Equation 1, the power input Q must be known. If Q cannot be measured directly, measurements of the temperatures in the specimen as it cools after the power is switched off (the recovery phase) can be used to determine the heat transfer coefficient between the top of the soil and the air, and hence the power. This approach, proposed by Clarke et al (2008), uses the lumped capacitance method, which assumes that the temperature difference across the length of the soil specimen is small compared to the temperature difference between the soil and the ambient air. The lumped capacitance method should only be used when the Biot number, Bi, (Equation 2) is small (Incropera et al, 2007):

$$\boldsymbol{\frac{T_{base} - T_{top}}{T_{top} - T_{amb}} = Bi < 0.1} \qquad \textbf{Equation 2}$$

where subscripts `base', `top' and `amb' refer to the temperature at the base of the soil, top of the soil, and of the ambient air respectively. The ambient temperature is assumed to be constant. The Biot number, Bi, is a dimensionless group quantifying the ratio of resistances to heat transfer by conduction and convection. Where Equation 2 is satisfied, the temperature of the soil at time, t, is (Clarke et al, 2008):

$$\boldsymbol{T = T_{amb} + (T_0 - T_{amb}) exp\left(-\frac{hA}{mc_p} t\right)} \qquad \textbf{Equation 3}$$

where T_0 is the temperature of the soil at time t=0 (when Equation 2 starts to apply), h is the convective heat transfer coefficient, m is the total mass of soil, and c_p is the soil specific heat capacity. The specific heat capacity is estimated from the mass-weighted properties of the soil constituents:

$$\boldsymbol{mc_p = m_s c_{ps} + m_w c_{pw}} \qquad \textbf{Equation 4}$$

where subscripts `s' and `w' refer to soil particles and water respectively. Equation 3 gives a theoretical decay curve which can be fitted to the experimental data by modifying h until the two curves match. At steady state, conservation of energy requires that the heat flow rate across the soil is equal to the heat flow rate at the top of the specimen from the soil to the air:

$$\boldsymbol{Q = \lambda A \frac{T_{base} - T_{top}}{L} = hA\left(T_{top} - T_{amb}\right)} \qquad \textbf{Equation 5}$$

This is used to calculate the thermal conductivity. It is worth mentioning that this method introduces an error associated with the estimation of the bulk specific heat capacity from those of the soil constituents (Equation 4), whose properties may not be accurately known.

3 Laboratory tests

3.1 Method

For clarity, the thermal cell used in this research will hereafter be referred to as the UoS (University of Southampton) thermal cell, and the thermal cell from (Clarke et al 2008) as the Clarke thermal cell. Figure 1 shows how they differ. Most notably, the UoS cell has a thicker acrylic base and thicker insulation in an attempt to minimise unwanted heat losses. The UoS cell uses expanded polystyrene as the insulation as it has a low thermal conductivity and could be easily wrapped around the soil specimen.

The top platen in the Clarke cell was used to maintain a constant temperature at the top of the specimen if a constant ambient air temperature could not be maintained. This platen was removed from the UoS cell as testing was conducted in a temperature controlled room. Instead the top of the specimen was covered with a sheet of aluminium foil to prevent the soil from drying. To measure the temperature at the top of the soil, a thermistor was mounted inside the tip of a hypodermic needle and inserted 2mm into the top of the soil, at the centre of the specimen cross-section (Figure 2).

Clarke et al (2008) monitored the temperature gradient within the specimen by pushing two hypodermic needle thermistors radially into the specimen at a height of one third and two thirds of the total height. The UoS cell did not have these additional thermistors, as the soils were too hard for the hypodermic needles to be inserted. Even if this were not the case, the needles would cause additional disturbance to the soil and require holes in the insulation for insertion the needles, potentially forming thermal bridges.

Tests were carried out on six samples of London Clay taken from different depths within a ground investigation borehole at a central London development site. Prior to the thermal cell tests, the thermal conductivities of the samples were measured with a needle probe (Hukseflux Thermal Sensors2003), which is a standard transient method. The results from these tests (Low et al, 2015, Low, 2016) were used in the thermal cell numerical models (see Section 4.2.2).

Two 100 mm long specimens were cut from each sample; hereafter these are referred to as `top half' and `bottom half' for each depth. To carry out a test, the cartridge heater was turned on and the power controlled so that the platen remained at a constant temperature of 40^{o}C. Temperatures were monitored until a steady state was reached, and maintained for a period of at least 2 hours. The power to the cartridge heater was then switched off, and the temperature during the recovery period monitored.

In contrast to the examples presented in Clarke et al (2008), in none of twelve London Clay tests were the temperatures at the top and bottom of the soil similar during recovery. Therefore, the Biot number never fell below 0.1 and the power could not be calculated using the lumped capacitance method. Instead the applied power had to be measured directly. The data logger was programmed to record when the cartridge heater switched on and off. The average power applied during the steady state stage could then be calculated from the known cartridge heater power of 50 W.

3.2 Results

A typical test result is shown in Figure 3. Table 2 shows the specimen properties at steady state and the calculated thermal conductivity. The thermal conductivities for all the specimens are shown in Table 3 and are within the expected range for London Clay (e.g. Banks et al, 2013).

While the experiments were fairly straightforward and the data simple to interpret, the results were consistently higher than those determined using the needle probe apparatus (Low et al, 2015, Low, 2016). This led to concerns about heat losses through the acrylic base and insulation, which are investigated in the following section.

4 Numerical modelling

Potentially the greatest source of error in the thermal conductivity method is in determining the power input. The interpretation of the experimental results described above does not take into account any heat losses that may occur through the base and insulation. Numerical modelling using the finite element software COMSOL was used to determine the significance of this effect. Three models were constructed to represent: (a) the UoS cell, (b) the Clarke cell, and (c) an ideal lossless cell. The models were 2D axisymmetric, and assumed no change in thermal properties of the materials with temperature. The models were used to determine the heat losses, and to discover why the UoS temperature decay data did not satisfy the criterion for using the lumped capacitance method, while that given in Clarke et al (2008) appears to have done so.

4.1 Modelling heat transfer

Heat transfer in a solid is governed by the heat diffusion equation:

$$\boldsymbol{\rho c_p \frac{\delta T}{\delta t} - \nabla \cdot (\lambda \nabla T) = \dot{Q}} \qquad \textbf{Equation 6}$$

where ρ is the mass density, c_p is the heat capacity, T is temperature, t is time, λ is the thermal conductivity, and $\dot{Q}$ is the heat flux per unit volume.

The three models were meshed using triangular elements of maximum size 2 mm. Mesh sensitivity using a heat balance was carried out that showed this degree of discretisation produced >99.7% of the expected result and was therefore acceptable.

4.2 UoS thermal cell

The model of the UoS thermal cell is shown in Figure 4a. The following sections outline how the properties of the model were chosen. Steady state and transient simulations were carried out, depending on the required output. For the steady state analysis, a constant power was specified for a heat source in the aluminium platen, simulating the cartridge heater. Alternatively, a constant temperature condition at the

top of the platen could be used. For the transient analysis, a constant heat source would be unrepresentative of the actual thermal cell, because the power varies initially to maintain a constant temperature of 40°C. Therefore, the heat source was replaced by a constant temperature condition at the top of the platen during the heating phase, which was disabled during the recovery phase. Heat losses and the suitability of the lumped capacitance method were investigated using these transient simulations.

4.2.1 Material properties

Unless stated otherwise, the material properties used in the models were as shown in Table 4. The ambient temperature and the initial temperature of the thermal cell were the same, 20°C.

4.2.2 Heat transfer coefficient

The external boundary conditions were all assumed to be convective with the heat flux at the boundary determined by a heat transfer coefficient, h (W/m^2K). The heat transfer coefficient between the top and sides of the UoS thermal cell and the surrounding ambient air had to be determined. To do this, steady state analyses were run for heat transfer coefficients from 10 to 35 W/m^2K, with the temperature at the top of the platen set to 40°C. The temperature at the top of the specimen during steady state was obtained from the output. This was compared with the experimentally measured top temperature for the 8.00 - 8.45 m depth top specimen, and the 19.00 - 19.45 m depth top specimen. The soil thermal conductivities in the models were set to the values measured by the needle probe at the relevant depths, 1.32 W/mK and 0.96 W/mK respectively. The average heat transfer coefficient was found to be 15 W/m^2K, which was used in subsequent simulations.

During these simulations, the boundary between the thermal cell base and the laboratory bench on which it stood was modelled as convective with a heat transfer coefficient of 5 W/m^2K. A sensitivity study was carried out for this parameter, which was varied between 0 and 25 W/m^2K while the heat transfer coefficient at the other boundaries was set at 15 W/m^2K as determined previously. It was found that varying the base heat transfer coefficient had a negligible effect on the results, perhaps because of the relatively small surface area of the thermal cell in contact with the bench. Therefore, the initial assumption of 5 W/m^2K was maintained in subsequent simulations.

4.2.3 Heat losses

The main objective of the numerical simulation was to determine the significance of heat losses in the thermal cell laboratory tests. This was done using the steady state analysis. In the UoS thermal cell model, a constant power to the cartridge heater was specified (with the source located at the centre of the platen) and adjusted until a soil base temperature of 40°C was achieved, and the heat fluxes at the top and bottom of the soil at steady state were used to calculate an average heat flux through the soil. The thermal conductivity of soils tends to lie in the range of 0.2 to 5 W/mK (GSHPA, 2012). For this range, the power loss was calculated as:

$$\boldsymbol{Power\ loss}\ (\%) = \frac{\boldsymbol{Q}-(\boldsymbol{Q_{top}}+\boldsymbol{Q_{bottom}})/\boldsymbol{2}}{\boldsymbol{Q}} \times \boldsymbol{100} \qquad \textbf{Equation 7}$$

where Q is the total power supplied to the cartridge heater, and subscripts `top' and `bottom' refer to the heat flux at the top and bottom of the soil specimen respectively. Figure 5 shows that the power loss is significant, particularly for soils of low thermal conductivity, with power losses of between 35% and 75%. This makes it difficult to determine what value of power to use in thermal conductivity calculations for the actual thermal cell. Above 3.5 W/mK it may be possible to estimate the power going through the soil as 35% less than the power to the cartridge heater. Below 3.5 W/mK the power going through the soil is much more dependent on the soil thermal conductivity. For any soil, estimating the power going through the soil as 35% less than the power to the cartridge heater would be an improvement to the thermal conductivity calculation.

Figure 6a shows the temperatures in the thermal cell as an isothermal contour plot. The boundary heat fluxes were aggregated to determine where the heat was being lost; the results are shown in Figure 7 for a soil specimen of conductivity 2.75 W/mk. This indicates that heat is lost through both the insulation and the base. Although it might be possible to reduce heat loss through the insulation by using better materials or a vacuum, the base must provide a stable platform to support the other components, while having as low a thermal conductivity as possible. It would be difficult to find a material that performs better in these respects than acrylic, so it is unlikely that base heat losses would be further reduced with a similar specimen arrangement. This problem can be addressed by testing two specimens that sandwich the heater as in standard guarded hot plate method (BSI, 2001). However, this apparatus requires much larger specimen sizes and hence is not really suitable for soils. Nonetheless the principle can be adopted for soils in bespoke apparatus, e.g. Alrtimi et al (2013).

One possible way of reducing the radial heat loss is to reduce the thickness of the specimen. For a range of thicknesses, the power to the cartridge heater was varied until a base temperature of 40^{o}C was reached. The thermal conductivity was then calculated using the total power and temperature difference across the specimen (Figure 8). Errors do reduce for thinner specimens, but even for a thickness of 10 mm, the calculated thermal conductivity was significantly different from the thermal conductivity specified in setting up the model. Smaller thicknesses would not be feasible from an experimental point of view.

In experiments by Alrtimi et al (2013), a similar method of calculating the thermal conductivity at different specimen lengths was applied in practice. They extrapolated from these values to find the thermal conductivity for a theoretical zero length specimen. This should reduce the influence of radial heat losses on the calculated thermal conductivity, but considering the value of thermal conductivity at zero thickness from Figure 8 it is suggested that this approach cannot totally compensate for radial losses and that large errors may still remain.

4.2.4 Time-dependent response and recovery curve

The transient model was able to produce a time-dependent simulation of the UoS thermal cell for comparison with the experimental results (Figure 9). During the heating phase, the power to the cartridge heater was not constant but was varied to keep the temperature at the base of the soil constant. Therefore, to obtain a time-dependent result reflecting to the experimental setup, the constant power condition was replaced with a constant temperature boundary condition of 40°C applied at the base of the soil during the heating phase. During the recovery phase this constant temperature was disabled and the temperatures within the soil allowed to find their own equilibrium. All other external boundary conditions remained unchanged.

For the thermal cell tests on the London Clay samples, the recovery curve could not be used to estimate the power as the temperature difference across the soil was too large for the lumped capacitance method to apply. The Biot number during recovery is plotted for both the UoS thermal cell numerical model and for the laboratory test on the 8.00-8.45 m depth top specimen in Figure 10. The Biot number in the model was higher than in the laboratory test, and did not gradually decrease. This is because the recovery temperatures in the model decreased more rapidly than in the laboratory test, which could be due to imperfect contacts at boundaries in the test, such as between the soil and the insulation, which would slow the rate of temperature decrease. This effect can also be seen during the heating phase, where the top temperature rises more rapidly in the model. Alternatively, it may be that the thermal conductivity and heat transfer coefficient values used in the simulations do not match those in the real experiments. Despite the difference in shape of the two graphs, the Biot number never fell below 0.1 in either case. Therefore, the lumped capacitance method is not recommended for calculating the power in a UoS thermal cell test. The power should instead be measured directly.

4.3 Clarke thermal cell

In Clarke et al (2008) a theoretical decay curve was fitted to the recovery data to determine the power applied to the soil specimen. The temperature difference through the soil was small during recovery, allowing the lumped capacitance method to be used. A model of the Clarke cell was made (Figure 4b) to determine whether this could be the case, and how and why the recovery curve may differ from the UoS thermal cell. The model dimensions were the same as the Clarke cell (Figure 4), except for the removal of the top aluminium plate and platen. This was the configuration adopted for a test on saturated fine Leighton Buzzard sand (Clarke, 2015 pers. comm.), the result of which was given in Clarke et al (2008) and is used here for comparison. The material properties were assumed to be the same as in the model of the UoS cell, which were given in Table 4. The ambient temperature in the laboratory was approximately 12°C, less than that in the Southampton tests. This resulted in a lower specimen top temperature (30.6°C) for a comparable base temperature (40.8°C) at steady state.

The thermal conductivity of the soil in the model was set to 2.75 W/mK, which was measured by Clarke et al (2008) in their experiment using the thermal cell on a specimen of Leighton Buzzard sand. Clarke et

al (2008) assumed a heat transfer coefficient of 25 W/m^{2}K and initially this value was used on all external boundaries of the model. However, the shape of the resulting temperature-time graph was significantly different from the experimental data reported in Clarke et al (2008). The heat transfer coefficient and the thermal conductivity were individually varied until the experimental steady-state temperature of 30.6^{o}C at the top of the specimen was reached, to see if a closer fit could be achieved. This did not produce a graph that was similar to the experimental result. However, when both the soil thermal conductivity and the heat transfer coefficient were varied, a similar graph was achieved (Figure 11). Using this model, a significant portion of the recovery curve had a Biot number just above 0.1, as in Figure 12. It could be argued that based on this, it may be inappropriate to use the lumped capacitance method to determine the power input. Additionally, the model fit was only achieved by using a model thermal conductivity of 1.4 W/mK, compared with an experimental thermal conductivity of 2.75 W/mK. The fitted value of the heat transfer coefficient was 4.4 W/m^{2}K.

Compared with the recovery of the UoS thermal cell results, the top and base temperatures of the Clarke cell converge much more rapidly. This is possibly due to greater heat losses through the insulation and base, resulting in a more rapid decrease in temperature at the specimen base. The losses at steady state are shown in Figure 6b. The temperature of the acrylic base has been raised significantly by the power supplied to the cartridge heater.

The alternative to the lumped capacitance method would be to measure the power directly for use in the thermal conductivity calculation. However, the heat losses through the insulation and base in Figure 6 are clearly greater than those for the UoS thermal cell. Hence direct measurement of the heater power would lead to an incorrect calculation of the thermal conductivity unless losses accounted for specifically.

4.4 Ideal thermal cell

The lumped capacitance method was unsuitable for use with the UoS thermal cell due to the Biot number never falling below 0.1 during the recovery phase of the test. Numerical simulation of the Clarke thermal cell showed that the Biot number did approach 0.1 as the temperature in the soil specimen converged more rapidly during recovery. However, this superficially better fit to the lumped capacitance method is most likely to be caused by greater heat losses from the Clarke thermal cell compared with the UoS thermal cell.

To explore the effect of heat losses on the recovery phase of the test further and to examine whether the lumped capacitance method would ever be applicable, a further numerical model of a perfectly insulated thermal cell was produced (Figure 4c). At the base was a thin disk (1 mm thickness) with the same properties of the soil. This is because COMSOL could not model a boundary with a constant temperature condition that was also perfectly insulating. Therefore, a constant temperature condition was defined at the top of the disk, and the base was perfectly insulated. The upper surface of the specimen was retained as a convective boundary condition with an assumed heat transfer coefficient of 25 W/m^{2}K.

The model was run for different values of soil thermal conductivity. For each value, a theoretical curve (see Equation 3) based on the lumped capacitance method was fitted to the numerical model recovery curve, and then the thermal conductivity was calculated based on the theoretical curve. The results of this analysis are shown in Figure 13. It can be seen that the higher the thermal conductivity, the more closely the theoretical curve resembles the model curve. Hence, the thermal conductivity calculated using the theoretical curve becomes closer to the model value as the thermal conductivity increases, as shown in Figure 14. Calculation of the minimum Biot number for each simulation shows how this decreases as the thermal conductivity increases (Figure 14). Furthermore, errors in thermal conductivity determination of less than 10% are only obtained once the Biot number has fallen below a value of 0.1 which occurs at approximately 13 W/mK thermal conductivity.

Typically, soil thermal conductivity ranges between 0.2 and 5 W/mK (GSHPA, 2012). Within this range of soil thermal conductivities, the lumped capacitance method would give a significant underestimate of the thermal conductivity for an ideal thermal cell, according to the numerical analysis. Interestingly, the reason why the Biot number remains large is because of the lack of heat losses. The significant difference in temperature between the base and top of the soil specimen is due to the heat being dissipated much more rapidly from the top by convection, while the base has insulation on all sides slowing the rate of temperature decrease. Comparison of the results for the UoS, Clarke and ideal thermal cells shows that at realistic soil thermal conductivities increasing the heat losses improves the apparent fit of the response curve to the theoretical solution, albeit with the wrong parameter values. On this basis it might be argued that for a poorly insulated thermal cell, the power would be better estimated using the lumped capacitance method, and for a well insulated thermal cell the power should be measured directly. However, both these approaches have still be shown to lead to appreciable errors in the estimation of the specimen thermal conductivity. This demonstrates the difficulty of determining the correct power, and calls into question the validity of the thermal cell method.

5 Conclusions

Laboratory testing using a thermal cell based on the specification of Clarke et al (2008) has shown that the temperature difference across the soil is too great for the lumped capacitance method to be used during the recovery phase as a means of calculating the power. The power should instead be measured directly, for example using the data logger to record when the cartridge heater was switched on and off.

Numerical modelling has shown that the UoS thermal cell has significant heat losses of at least 30% over the range of typical soil thermal conductivities. This would impact the thermal conductivity calculated from a laboratory test. Similarly, the numerical model showed a significant temperature difference across the soil during the recovery phase of the test, confirming that the lumped capacitance method was not appropriate. A second numerical model simulating the Clarke cell also showed this to be the case.

Analyses using a numerical model of an ideal (perfectly insulated) thermal cell showed that for the range of soil thermal conductivities, the lumped capacitance method would give a significant error in the calculated thermal conductivity. Only for thermal conductivities above 15 W/mK did this error fall below 10%.

This research has shown that neither the UoS nor Clarke thermal cells give accurate results because of the significant and unavoidable effects of heat losses. The heat losses vary depending on the type of soil, with the lowest thermal conductivity soils having the highest heat losses, potentially over 50%. Even for quartz rich higher thermal conductivity soils heat losses will always exceed 30% for the types of thermal cell examined. The lumped capacitance method is unlikely to be applicable for realistic soil thermal conductivities since the approach only gives an apparently good fit to the theoretical curve on a cell with significant heat losses and in such cases the parameter values are then wrong. If the power could be measured directly, eliminating the need for the lumped capacitance method, and heat losses were drastically reduced, a more accurate thermal cell could be developed. However, arrangements similar to those presented in this paper potentially lead to significant errors in thermal conductivity determination. Hence transient measurement methods are preferable if heat losses cannot be controlled sufficiently.

Acknowledgements

The authors would like to thank Harvey Skinner for his help in the design, build, and instrumentation of the apparatus. The soil samples were provided by Concept Engineering Consultants Ltd and Arup. We are grateful for the site support from Canary Wharf Contractors Ltd, and Marton Geotechnical Services Ltd. This work forms part of a larger project funded by EPSRC (ref EP/H0490101/1) and supported by Mott MacDonald Group Ltd, Cementation Skanska Ltd, WJ Groundwater Ltd, and Golder Associates. The second author also gratefully acknowledges subsequent financial support from the Royal Academy of Engineering.

References

Alrtimi AA, Rouainia M and Manning DAC (2013) Thermal enhancement of PFA–based grout for geothermal heat exchangers. Applied Thermal Engineering 54: 559–564.

Banks D (2008) An introduction to thermogeology: ground source heating and cooling. Blackwell Publishing Ltd.

Banks, D., Withers, J. G., Cashmore, G., & Dimelow, C. (2013), An overview of the results of 61 in situ thermal response tests in the UK, Quarterly Journal of Engineering Geology & Hydrogeology, 46, 281-291.

Bristow KL, Kluitenberg GJ and Horton R (1994) Measurement of Soil Thermal Properties with a Dual-Probe Heat-Pulse Technique. Soil Science Society of America Journal 58: 1288–1294.

BSI (2001), BS EN 12667:2001 Thermal performance of building materials and products – Determination of thermal resistance by means of guarded hot plate and heat flow meter methods – Products of high and medium thermal resistance, BSI, London.

Clarke BG, Agab A and Nicholson D (2008) Model specification to determine thermal conductivity of soils. Proc ICE Geotechnical Engineering 161: 161–168.

Farouki O (1986) Thermal properties of soils. Series on rock and soil mechanics, Trans Tech.

GSHPA (2012) Thermal Pile Design, Installation & Materials Standards. Ground Source Heat Pump Association, Milton Keynes.

Hukseflux Thermal Sensors (2003) TP02 Non-Steady-State Probe for Thermal Conductivity Measurement – manual v0908. Hukseflux Thermal Sensors, Delft.

Incropera FP, DeWitt DP, Bergman TL and Lavine AS (2007) Fundamentals of Heat and Mass Transfer. 6 edn., John Wiley & Sons Inc.

Jablite Intelligent Insulation (2014) Jablite Classic Expanded Polystyrene Technical Information. http://www.jablite.co.uk/site/datasheets/6/6.pdf.

Low, J. E. (2016) Thermal conductivity of soils for energy foundation applications, PhD thesis, University of Southampton.

Low, J. E., Loveridge, F. A., Powrie, W. & Nicholson, D., 2015. A comparison of laboratory and in situ methods to determine soil thermal conductivity for energy foundations and other ground heat exchanger applications, Acta Geotechnica 10(2), 209–218.

Mitchell JK and Kao TC (1978) Measurement of soil thermal resistivity. Journal of the Geotechnical Engineering Division 104: 1307–1320.

Table 1 Dimension of UoS Thermal Cell

Material	**Dimensions (cm)**
Acrylic base	8.8 (maximum, at centre) x 15
Soil Specimen	10 x 10
Insulation	18 (height) x 7 (radial thickness)

Table 2 Example Results for the Thermal Cell Test

Sample Depth (m)	8.00 – 8.45
Specimen	Top half
Diameter (mm)	103
Length (mm)	106
Base temperature (^{o}C)	40.1
Top temperature (^{o}C)	28.4
Power (W)	1.85
Thermal Conductivity (W/mK)	**2.01**

Table 3 Thermal Cell Thermal Conductivity Results for all London Clay Samples

Sample Depth (m)	**Thermal Conductivity (W/mK)**	
	Top Half Specimen	**Bottom Half Specimen**
2.00–2.45	1.86	1.72
8.00–8.45	2.01	1.88
10.00–10.45	1.85	1.91
17.00–17.45	1.92	1.88
19.00–19.45	1.65	1.75
21.50–21.95	2.19	1.84

Table 4 Model Material Properties

	Soil[1]	Aluminium	Acrylic	Insulation[2]
Thermal conductivity (W/mK)	2.75	160	0.18	0.03
Specific heat capacity (J/kgK)	1632	900	1470	1130
Density (kg/m^3)	2010	2700	1190	23

1. Clarke et al, 2008; 2. Jablite Intelligent Insulation, 2014)

Figure 1 Cross section diagrams of a) the University of Southampton (UoS) thermal cell; and b) the Clarke thermal cell. In both cases the heat source is a cartridge heater embedded within the lower aluminium platen.

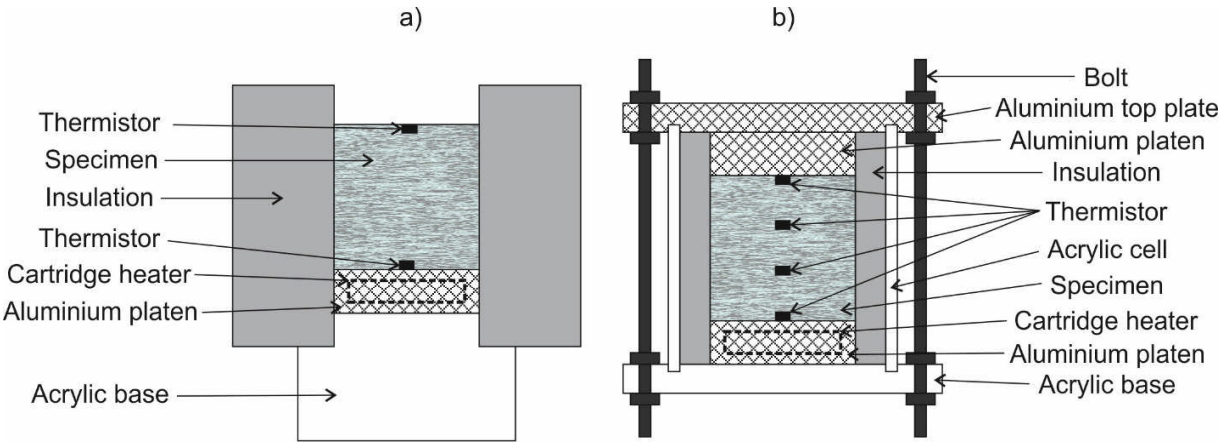

Figure 2 The UoS thermal cell showing the entire cell with insulation (left) and the base only (right)

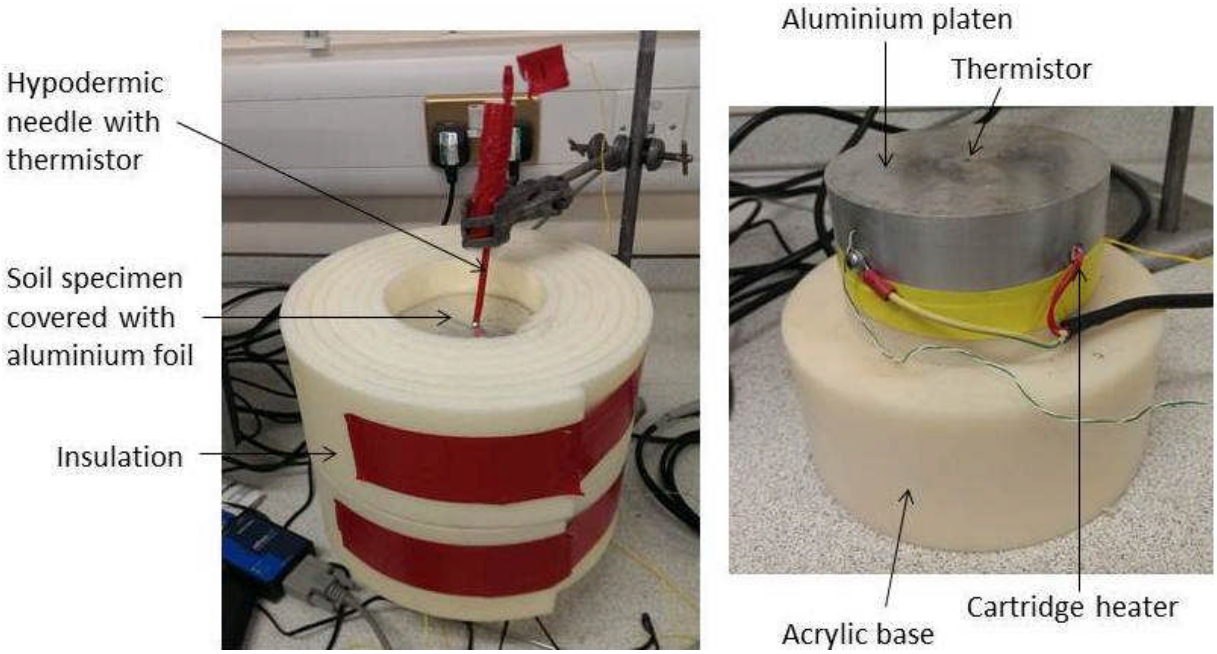

Figure 3 Thermal cell results for the top half of the 8.00 – 8.45m depth sample showing the measured temperatures and the calculated Biot number during recovery.

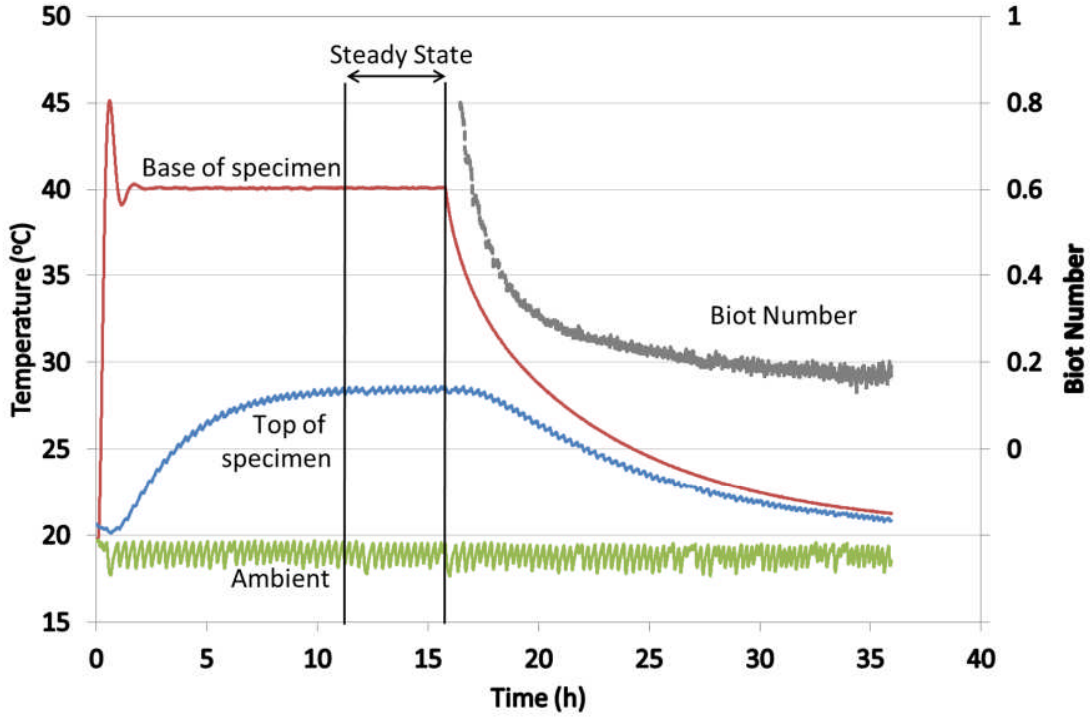

Figure 4 Model cross section showing materials and boundary conditions a) UoS thermal cell; b) Clarke thermal cell; c) idealised (perfectly insulated) cell.

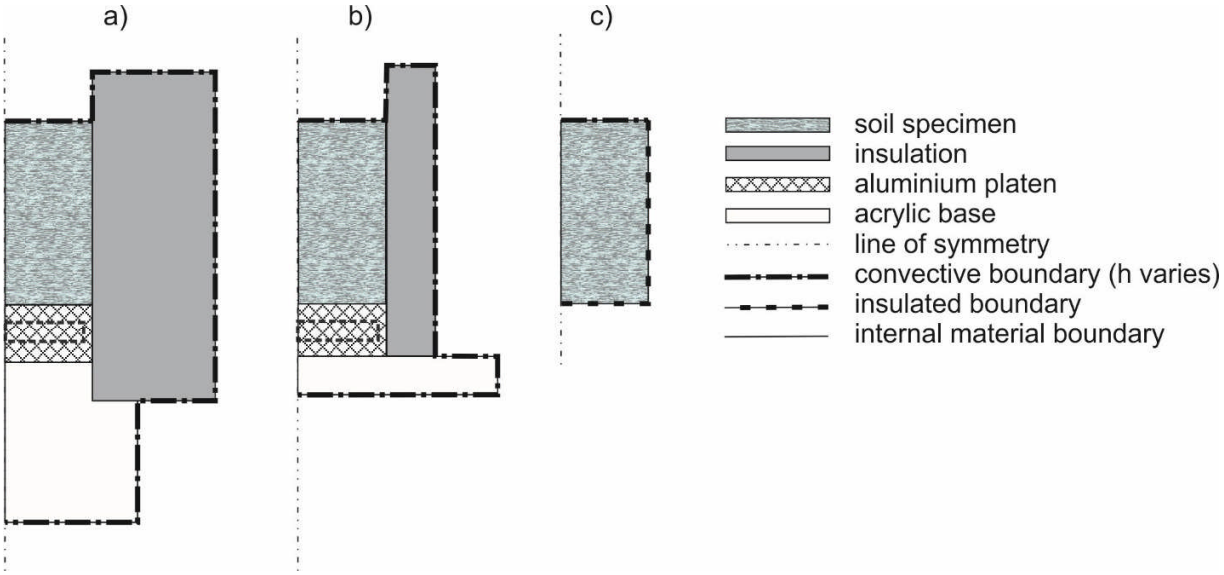

Figure 5 UoS thermal cell model: power loss for different soil thermal conductivities

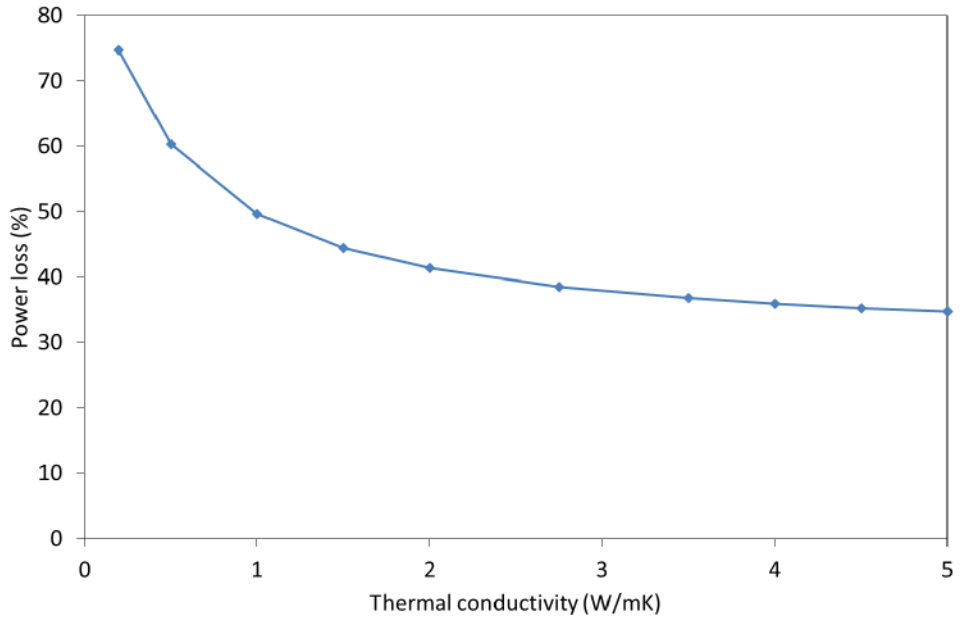

Figure 6 Numerical model results showing isothermal contours at 2°C intervals for soil thermal conductivity of 2.75 W/mK a) the UoS thermal cell; b) Clarke cell. In both cases the direction of heat flow is shown by arrows with lengths proportional to the relative heat flux magnitude.

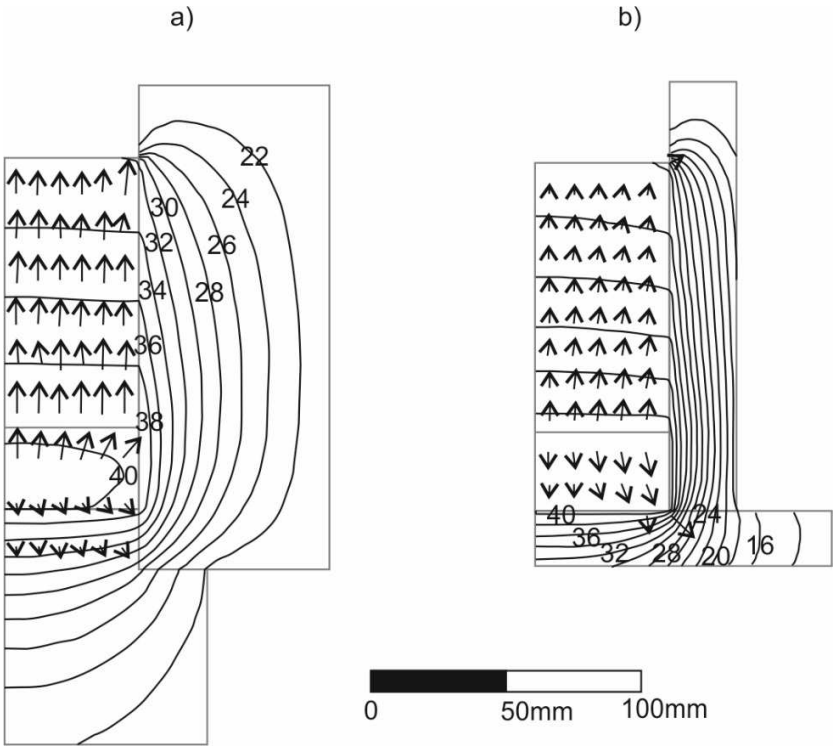

Figure 7 Heat flow balance for the modelled UoS thermal cell assuming a soil thermal conductivity of 2.75 W/mK. The total heat is supplied by the cartridge heater at A.

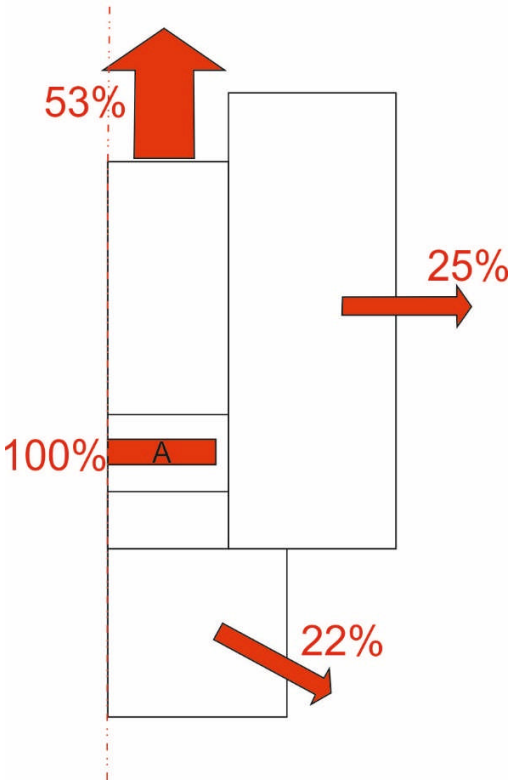

Figure 8 Calculated soil thermal conductivity for specimens of different thickness, based on the UoS thermal cell model, with a specified soil thermal conductivity of 2.75 W/mK.

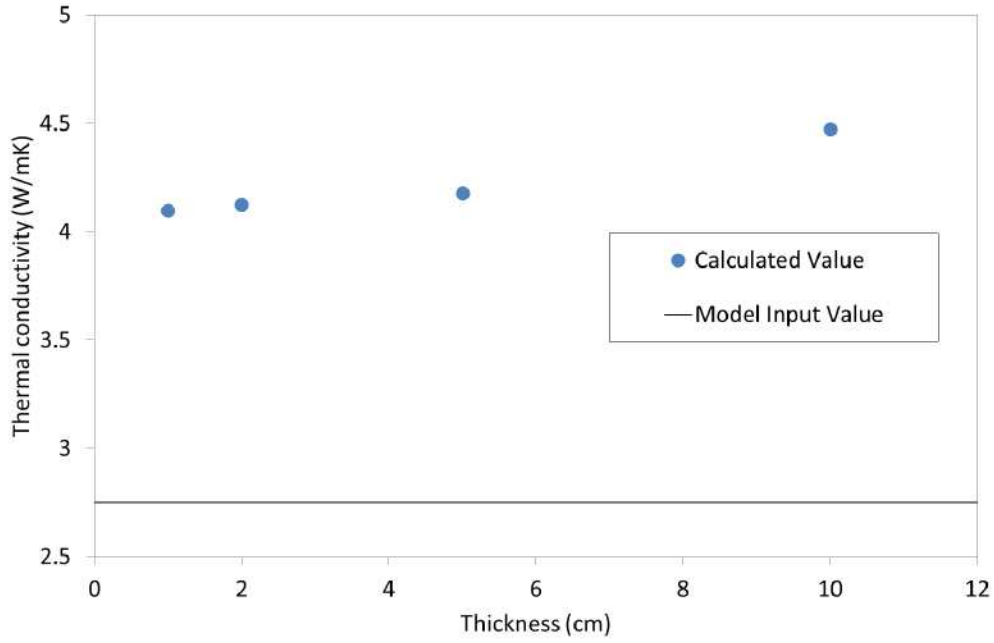

Figure 9 Comparison of the laboratory and modelled temperature variation with time for the UoS thermal cell for the 8.00 – 8.45m depth top specimen. Model assumes a soil thermal conductivity of 1.32 W/mK.

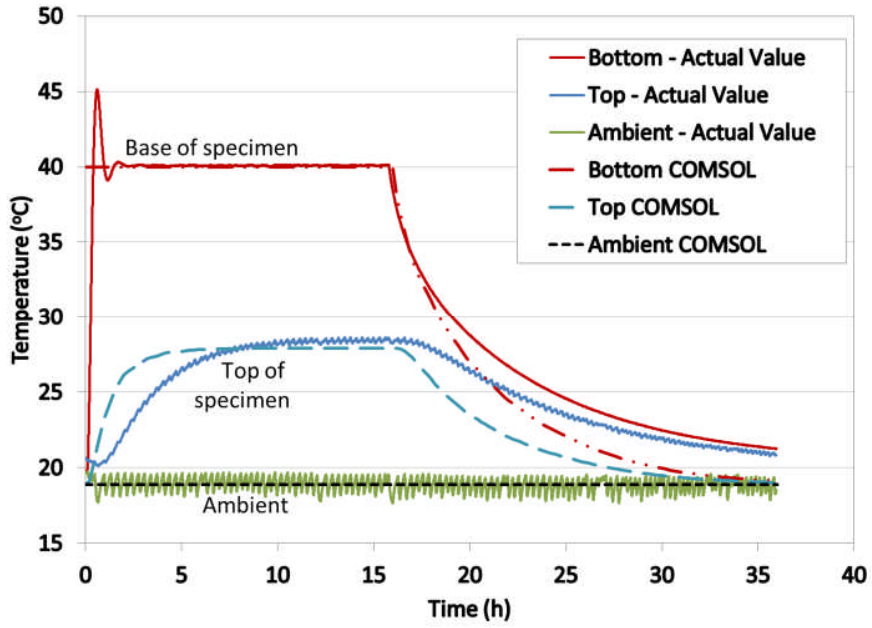

Figure 10 Comparison of the laboratory and modelled Biot number over time for the UoS thermal cell for the 8.00 – 8.45m depth top specimen. Model assumes a soil thermal conductivity of 1.32 W/mK.

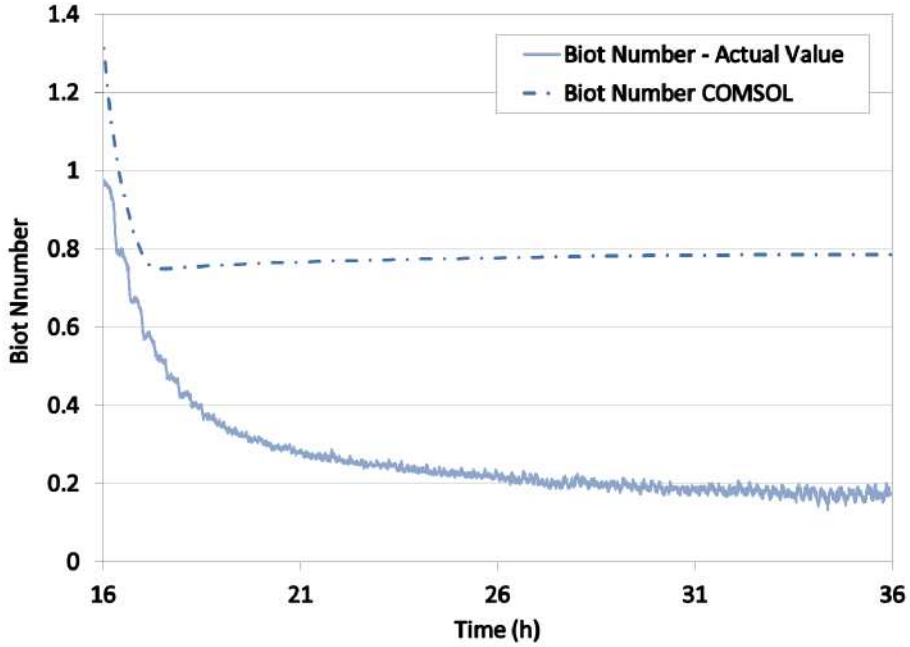

Figure 11 Comparison of the laboratory and modelled temperature variation with time for the Clarke thermal cell for Leighton Buzzard Sand assuming thermal conductivity of 1.4 W/mK and h=4.4 W/m^{2}K.

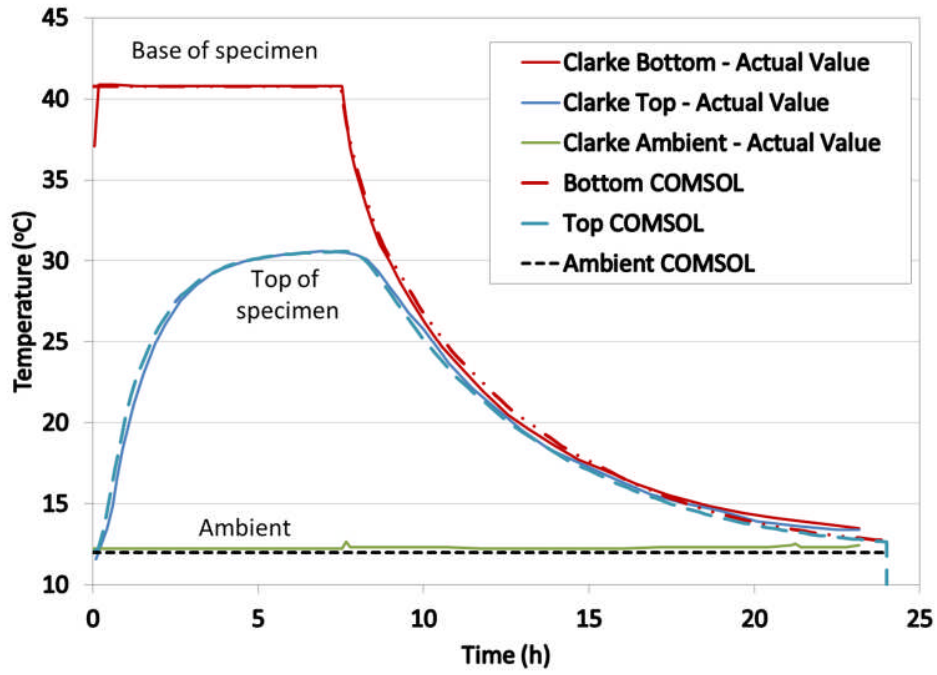

Figure 12 Modelled Biot number for the Clarke thermal cell for Leighton Buzzard Sand assuming a soil thermal conductivity of 1.4 W/mK and a top of specimen heat transfer coefficient of 4.4 W/m^{2}K.

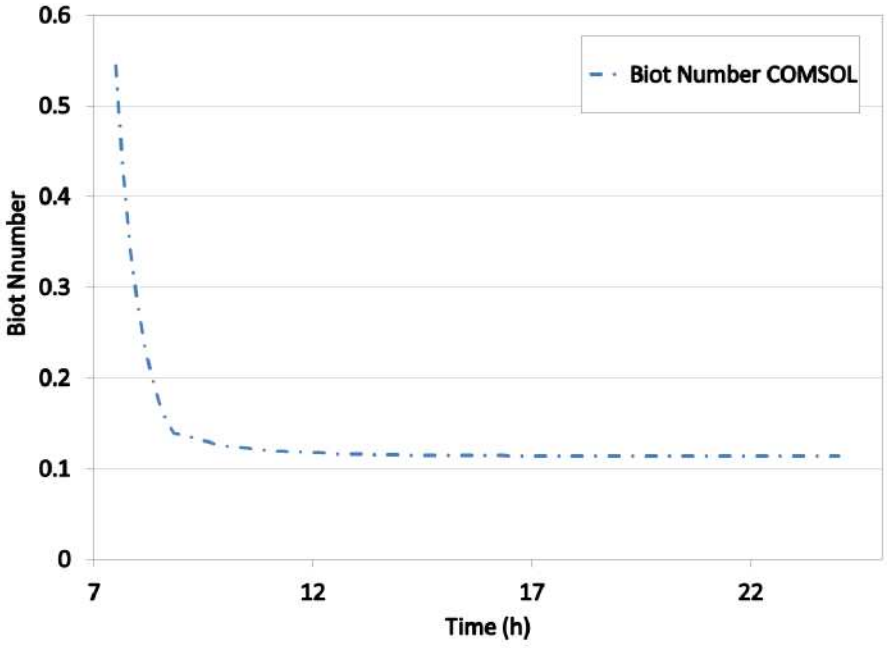

Figure 13 Recovery curves generated by the model idealised thermal cell compared with the theoretical fit curve for different values of soil thermal conductivity.

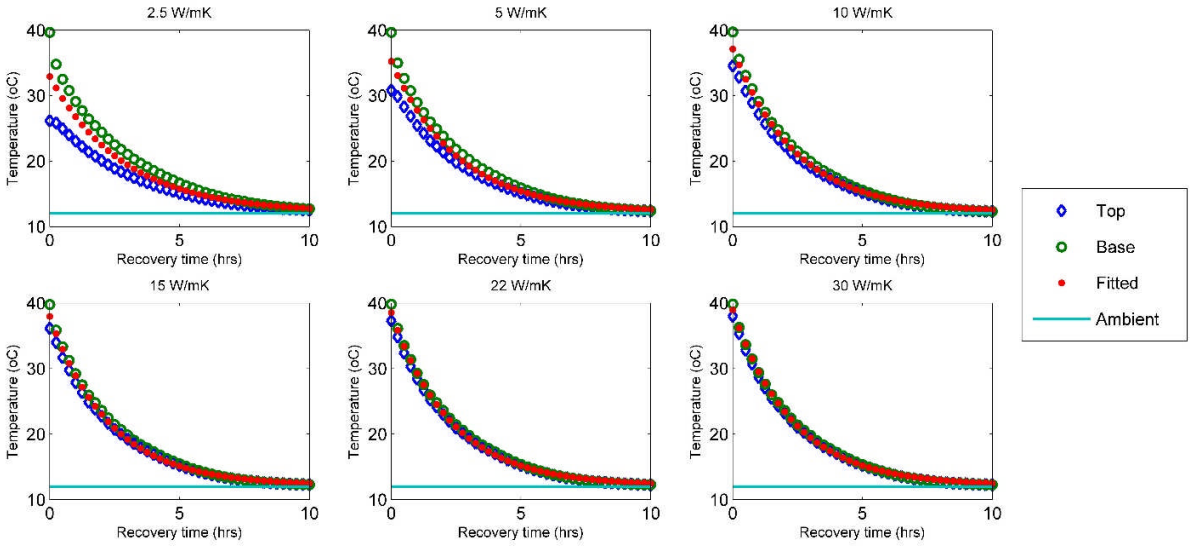
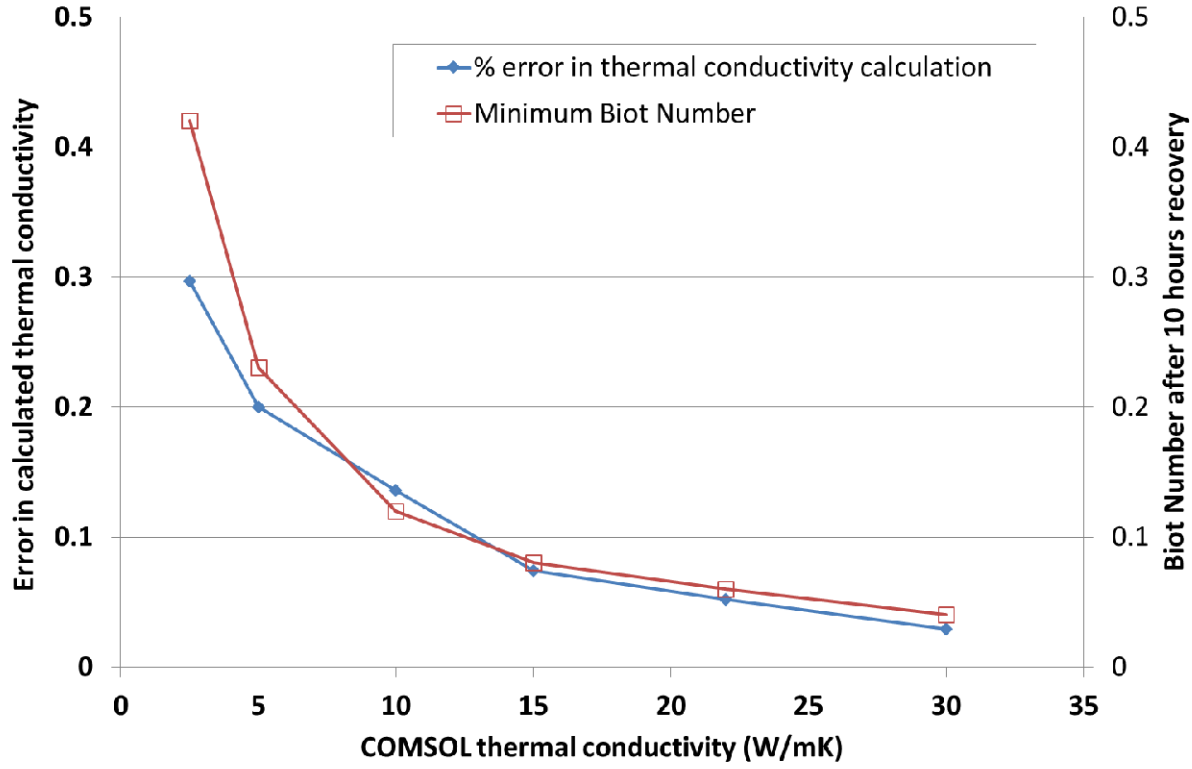
Figure 14 Error in calculated thermal conductivity using the lumped capacitance method, expressed as a percentage of the specified model thermal conductivity assuming an idealised (perfectly insulated) thermal cell.